The Effects of UV Aging on the Cracking of Titanium Oxide Layer on Poly(ethylene terephthalate) Substrate

Preprint

Chao Zhang, Matthew H. Gray, Robert Tirawat, and Ross E. Larsen
National Renewable Energy Laboratory

Fangliang Chen
Columbia University

Presented at the ASCE Earth and Space Conference 2016
Orlando, Florida
April 11–15, 2016

NREL is a national laboratory of the U.S. Department of Energy
Office of Energy Efficiency & Renewable Energy
Operated by the Alliance for Sustainable Energy, LLC

This report is available at no cost from the National Renewable Energy Laboratory (NREL) at www.nrel.gov/publications.

Conference Paper
NREL/CP-2C00-65867
April 2016

Contract No. DE-AC36-08GO28308

NOTICE

This report is available at no cost from the National Renewable Energy Laboratory (NREL) at www.nrel.gov/publications.

Available electronically at SciTech Connect http:/www.osti.gov/scitech

Available for a processing fee to U.S. Department of Energy and its contractors, in paper, from:

U.S. Department of Energy
Office of Scientific and Technical Information
P.O. Box 62
Oak Ridge, TN 37831-0062
OSTI http://www.osti.gov
Phone: 865.576.8401
Fax: 865.576.5728
Email: reports@osti.gov

Available for sale to the public, in paper, from:

U.S. Department of Commerce
National Technical Information Service
5301 Shawnee Road
Alexandra, VA 22312
NTIS http://www.ntis.gov
Phone: 800.553.6847 or 703.605.6000
Fax: 703.605.6900
Email: orders@ntis.gov

Cover Photos by Dennis Schroeder: (left to right) NREL 26173, NREL 18302, NREL 19758, NREL 29642, NREL 19795.

NREL prints on paper that contains recycled content.

The effects of UV aging on the cracking of titanium oxide layer on poly (ethylene terephthalate) substrate

Chao Zhang[*1], Fangliang Chen[2], Matthew H. Gray[3], Robert Tirawat[4], and Ross E. Larsen[*5]

[1]Computational Science Center, National Renewable Energy Laboratory, 15013 Denver Parkway MS ESIF301, Golden, CO 80228; PH (303) 275-3278; email: chao.zhang@nrel.gov
[2]Department of Civil Engineering & Engineering Mechanics, Columbia University, 500 West 120th ST, 161 Engineering Terrace, New York, NY 10027; PH (509) 715-9198; email: fangliang.chen@columbia.edu
[3]Buildings and Thermal Systems Center, National Renewable Energy Laboratory, 15013 Denver Parkway MS FTLB3321, Golden, CO 80228; PH (303) 275-3917; email: matthew.gray@nrel.gov
[4]Buildings and Thermal Systems Center, National Renewable Energy Laboratory, 15013 Denver Parkway MS FTLB3321, Golden, CO 80228; PH (303) 384-6360; email: robert.tirawat@nrel.gov
[5]Computational Science Center, National Renewable Energy Laboratory, 15013 Denver Parkway MS ESIF301, Golden, CO 80228; PH (303) 275-4422; email: ross.larsen@nrel.gov

ABSTRACT

Thin oxide and metal films deposited on polymer substrates are emerging technologies for advanced reflectors for concentrated solar power applications, due to their unique combination of light weight, flexibility and inexpensive manufacture. Thus far, there is little knowledge on the mechanical integrity or structural persistence of such multi-layer thin film systems under long-term environmental aging. In this paper, the cracking of a brittle titanium dioxide layer deposited onto elasto-plastic poly(ethylene terephthalate) (PET) substrate is studied through a combination of experiment and modeling. *In-situ* fragmentation tests have been conducted to monitor the onset and evolution of cracks both on pristine and on samples aged with ultraviolet (UV) light. An analytical model is presented to simulate the cracking behavior and to predict the effects of UV aging. Based on preliminary experimental observation, the effect of aging is divided into three aspects and analyzed independently: mechanical property degradation of the polymer substrate; degradation of the interlayer between substrate and oxide coating; and internal stress-induced cracks on the oxide coating.

INTRODUCTION

The development of advanced collectors with high reflectivity, low cost and long lifetimes is one of the barriers for the expanded application of concentrated solar power. While the traditional solar reflectors (Design A of Figure 1) utilizing silver painted on back of glass is known to have good stability over time, advanced front

surface designs (Design B of Figure 1) that combine a flexible polymer film with protective top coats and a UV-screening material on top of the film attain high reflectance and lower cost. However, one issue with the polymer based reflector system is its long-term aging performance (scheme of Figure 1), as it is more likely to be degraded due to the diffusion of oxygen and moisture into the system and subsequent chemical reactions (DiGrazia et al. 2012). Also the resultant transverse cracking and interface damage events under mechanical loads from, e.g., wind, could cause catastrophic failure of the protective coatings, leading to, for example, water infiltration and subsequent rapid reduction of the reflectance.

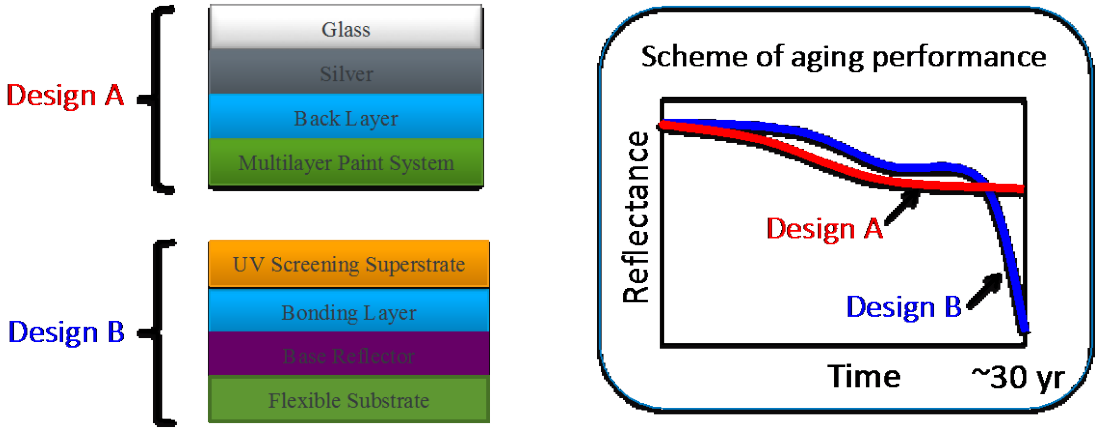

Figure 1: Schematic reflector designs and their aging performance.

Due to the brittle nature of the thin oxide films, cracks will initiate in the coating layer at a very low strain level (less than 1%) as reported by Leterrir (2003) and Yanaka et al. (1998). Leterrier et al. (1997) conducted a series of fragmentation tests on SiO_x coating on the poly(ethylene terephthalate) (PET) substrate and found that the crack density could be as high as 400 /mm (corresponding to a crack space of 2.5 μm) under a 20% normal tensile strain. The initiation of cracks in the thin film will result in an increase of surface roughness and permeability of the protective coating layer, a decrease of transparency and a decrease in fracture tolerance. These will influence significantly the efficiency and sustainability of the multi-layered structure, especially under aging conditions that combine ultraviolet (UV) irradiation, humidity and thermal cycling, etc. Thus, the understanding the cracking mechanism of thin film bonded polymer substrate is of great importance for the studying of aging performance of advanced solar reflector structure.

The cracking of bi-layer thin film coated on a ductile substrate has been extensively studied both experimentally and theoretically. A uniaxial fragmentation test is widely used to evaluate the coating fracture properties and interface properties between the coating and the substrate (Leterrier et al. 1997a and 1997b, Yanaka et al. 1998, Xia and Hutchinson 2000, and Xie and Tong 2005). Theoretically, linear elastic fracture mechanics (LEFM) models have been successfully employed to coating cracking analysis under uniaxial loading, for example, a shear lag model adopted by Laws and Dvorak (1988) and a variational model by Nairn and Kim (1992). Hu and Evans (1989) took into account the interface yielding by assuming it is controlled by a

constant shear stress. The role of the interface has been further studied by Li and Suo (2006, 2007) for a thin metal film on elastomer and ductile substrates using finite element methods. Recently, Chen et al. (2015) developed a one-dimensional elasto-plastic model, which solves explicitly the opening-mode fractures for an alumina coating fully bonded to an aluminum substrate undergoing large tensile deformation.
In the present paper, we investigate the cracking mechanism of a bi-layer thin film structure, titanium oxide (TiO_2) bonded on PET substrate, with a focus on the effect of photodegradation (UV aging) on the mechanical and physical properties of this multilayer structure. Polymer films are known to be sensitive to environmental aging, under which the mechanical toughness decreases continuously and the film becomes brittle after a certain aging time (Oreski and Wallner 2005). Consistent with the degradation of substrate properties, it is expected that the interface properties will change as well. Also, cracks may initiate due to aging-induced internal stress. In this paper, we conduct extensively *in-situ* fragmentation tests to monitor the onset and evolution of cracking phenomena. An analytical model is built to analyze the cracking behavior and correlate with experimental results. The correlated model is then employed to study the effect of UV aging through three aspects: mechanical property degradation of the polymer substrate; degradation of the interface between substrate and oxide coating; and internal stress-induced cracks on the oxide coating.

EXPERIMENT

Specimen. The material system we are studying consists of a titanium dioxide thin film deposited on a PET subsrtate, prepared in the Advanced Optical Material for Concentrating Solar Power Lab of the National Renewable Energy Laboratory. The PET substrate is optically clear Mylar® with a thickness of 76.2 μm and the TiO_2 film thickness is 300 nm. The deposition of TiO_2 is done from electron beam evaporation of a Ti_3O_5 source in a background of oxygen. Base pressure of the deposition system is 3.0×10^{-8} Torr. During evaporation a flow of O_2 maintains a pressure of 3.0×10^{-5} Torr. Sample surface temperatures are ambient resulting in amorphous films. The bi-layer coated specimens were cut into a rectangular shape with dimensions 50.4 mm in length and 10.16 mm in width (2 inch by 0.4 inch). PET substrate specimens (without TiO_2 film) of thickness 177.8 μm, Melinex® ST504, were also prepared to characterize uniaxial tensile properties.

Uniaxial tensile tests of UV aged PET film. To evaluate the evoultion of mechanical properties of the PET substrate under UV aging, uniaxial tensile tests of the PET with different UV exposure time were conducted using an Instron machine under a constant stretching speed of 3 mm/min. The tensile behavior of PET is known to be anisotropic with different responses along roll direction and transverse direction. In this work, all tests are performed along the roll direction. The PET films were aged at room temperature and ambient humidity at approximately 10 times the solar UVA/UVB light intensity for up to 96 hours. Figure 2 shows the tensile engineering stress-strain curves for PET substrate with UV exposure time of 0, 12, 24, 36, 48 and 78 h. From Figure 2, it is found that with the increase of exposure time the ultimate failure strain decreases significantly. When the UV exposure time goes beyond 48

hours, the PET film becomes brittle without any plastic deformation. On the other hand, the modulus and yield stress do not change appreciably during the aging.

***In-situ* fragmentation test of TiO_2 bonded on PET substrate.** Fragmentation tests were conducted to inversitigate the damage processes of the TiO_2/PET film, and more specifically, the crack evolution behavior of the TiO_2 layer. In these *in situ* tests, the evolution of crack patterns in the brittle coating was monitored using an optical microscope, during the uniaxial tensile loading applied to the subsrate. The tensile test was conducted using an *in-situ* SEM tester (MTI Instruments Inc.) placed on the mechanical stage of the microscope. A displacement controlled load with a rate of 0.1 mm/min was applied to the rectangular TiO_2/PET specimens until a maximum displacement of 2 mm. We noted that under a continuous loading situation, it is difficult to focus the microscope if the loading rate is too fast, while a slow loading rate, 0.1 mm/min, allowed us to accurately capture the crack pattern. The gauge section length of the specimens was about 25-30 mm after clamping the two ends with fixtures. Figure 3 shows a representative stress-strain curve of TiO_2/PET with a coating thickness of 300 nm and corresponding crack patterns at different strain levels. The first crack was observed at a strain level of 0.42%, which provides a upper bound of the crack onset strain. At such a low strain level, the crack presented very lightly on the coating layer, which is hard to elaborate through image due to the limitation of visulization technology. Obvious channeling cracks were formed at a strain level of 0.96% as shown in Figure 3, with an average crack space of 15.3 μm. An inclined crack at the left side was also observed, which is a crack that was present after the initial deposition. The crack space then decreases with the increase of strain and the saturated crack space is about 5.69 μm at a strain level of 5.6%.

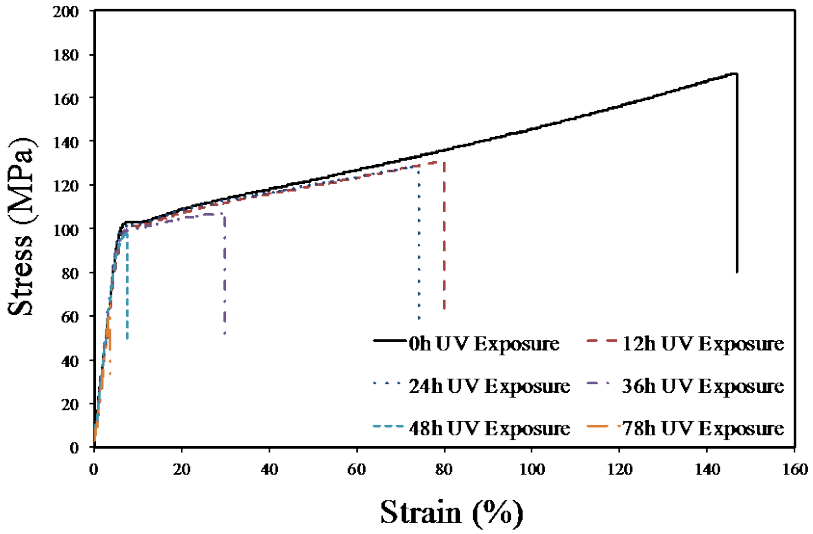

Figure 2: Experimental engineering stress-strain curves of PET film with different UV exposure times.

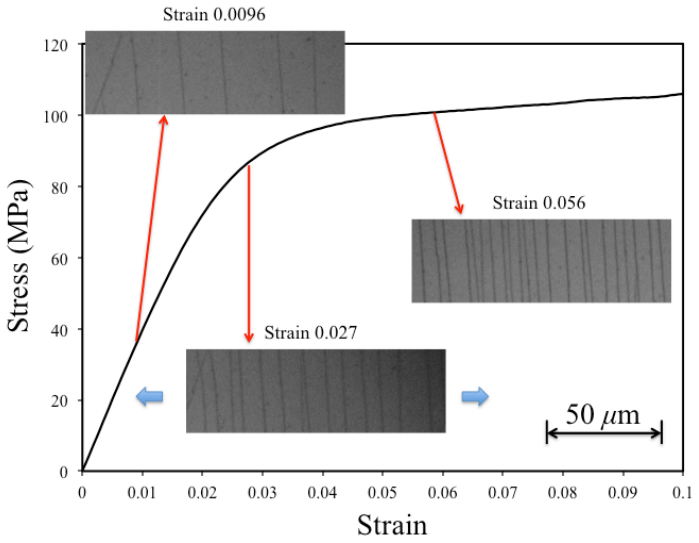

Figure 3: Stress-strain response and crack patterns at three different strain levels for TiO_2/PET with a coating thickness of 300 nm. The scale bar in the graph applies to the microscope images.

THEORY AND MODEL

The theoretical opening-mode fracture model developed by Chen et al. (2015) is applied in this study to investigate the crack onset and evolution in the thin film. We consider a brittle thin film (thickness h_f, length 2λ, Young's modulus E_f, Poisson's ratio v_f) fully bonded to a substrate (thickness h_s, Young's modulus E_s, Poisson's ratio v_s) and subjected to a uniform tensile load. A plane strain formulation is used for the constitutive law. Coordinate x denotes the length and loading direction and z denotes the thickness direction. Three different stress phases can be identified as the applied load increases: (1) linear elastic stage; (2) elasto-plastic stage; (3) opening-mode fracture stage. The explicit solutions of the stress and displacement in the first two phases and the energy release rate in the third phase are summarized as below:

Linear Elastic Stage. When the overall coating/substrate system is in the linear elastic range, the stress field will propotionally increase along with the tensile load. Following the procudure in (Yin and Prieto-Munoz, 2013), a general solution for displacement $u^f(x,z)$ and stress $\sigma^f(x,z)$ of the coating is obtained as

$$u^f(x,z) = A\cdot\cos(dh_f - dz)\sinh(cx) + \varepsilon_x^u x \tag{1}$$

$$\sigma^f(x,z) = \xi_f E_f[Ac\cdot\cos(dh_f - dz)\cosh(cx) + \varepsilon_x^u] \tag{2}$$

Using the shear stress continuity and interface continuity, the shear strain $\gamma^i(x)$ in the interlayer and displacement of substrate can be determined by

$$\gamma^i(x) = \frac{G_f}{G_i} Ad\cdot\sin(dh_f)\sinh(cx) \tag{3}$$

$$u^s(x) = A[-\frac{G_f}{G_i} dh_i\cdot\sin(dh_f) + \cos(dh_f)]\sinh(cx) + \varepsilon_x^u x \tag{4}$$

Since the thickness of the substrate is much larger than that of the coating and the interlayer, we can assume that the tensile load is approximately uniform in the thickness direction of the substrate layer. Solving a 1-D equilibrium equation, the stress $\sigma^s(x)$ in the substrate can be determined as

$$\sigma^s(x) = E_s\{Ac[-\frac{G_f}{G_i}dh_i \cdot \sin(dh_f) + \cos(dh_f)]\cosh(cx) + \varepsilon_x^u\} \tag{5}$$

In the above equations, $\xi_f = 1/(1-\nu_f^2)$, G_f and G_i are the shear modulus of thin film and interlayer, respectively. The coefficients c, d, A and ε_x^u are defined in Chen et al. (2015) and they are determined by the boundary conditions, such that A depends on λ.

Elasto-plastic Stage. As the applied load increases, yielding will begin in the interlayer and the substrate while the coating is still assumed to behave linearly. The previous analysis (Chen et al. 2015) suggests that the yielding initiates firstly in the interlayer at the two ends of span and then propagates toward the inner part. This indicates that the elasto-plastic range contains three stages: elastic substrate and elasto-plastic interlayer; plastic substrate and elasto-plastic interlayer; and plastic substrate and plastic interlayer. The formulations of solutions for the elasto-plastic range are similar to the linear elastic solutions, whereas the constitutive models for the interlayer and substrate have an isotropic linear hardening formation. The displacement and stress field in the coating/substrate system for the plastic substrate and plastic interlayer are shown below:

$$u^f(x,z) = B \cdot \cos(nh_f - nz)\sinh(mx) + \varepsilon_{x2}^u x \tag{6}$$

$$\sigma^f(x,z) = \xi_f E_f[Bm \cdot \cos(nh_f - nz)\cosh(mx) + \varepsilon_{x2}^u] \tag{7}$$

$$u^s(x) = B[-\frac{G_f}{G_i^t}nh_i \cdot \sin(nh_f) + \cos(nh_f)]\sinh(mx) + \varepsilon_{x2}^u x + h_i(\frac{1}{G_i^t} - \frac{1}{G_i})\tau_i^y \tag{8}$$

$$\sigma^s(x) = E_s^t\{Bn[-\frac{G_f}{G_i^t}nh_i \cdot \sin(nh_f) + \cos(nh_f)]\cosh(mx) + \varepsilon_{x2}^u\} + (1 - \frac{E_s^t}{E_s})\sigma_s^y \tag{9}$$

where G_i^t and E_s^t are the shear hardening rate and tensile hardening rate of the interlayer and substrate, τ_i^y and σ_s^y are the shear yield stress and tensile yield stress of interlayer and substrate. The coefficients m, n, B and ε_{x2}^u can be determined by the boundary conditions, such that B depends on λ, and are defined in Chen et al. (2015).

Opening-mode fracture stage. When the external tensile loading increases to a critical value, a new crack may nucleate along the central line of the coating. The normal stress along the central line just before the fracture can be obtained using Eq.(2) or (7). Once a new fracture forms, the section cracked into two pieces. The crack-opening displacement field can be solved by Eq.(1) or (6) replacing 2λ to λ. The energy release rate (ERR), G, by this fracture is the work done by the normal stress necessary to close the crack opening displacement (Beuth, 1992).

$$G = \frac{1}{2h_f}\int_0^{h_f} \sigma^f(0,z)u^f(0,z)dz \tag{10}$$

Beuth (1992) and Beuth and Klingbeil (1996) also proposed the ERR of a semi-infinite isolated crack for thin film bonded to elastic and elasto-plastic substrate as

$$G = \frac{1}{2}E_f(\varepsilon_{cr})^2\pi h_f g(\alpha,\beta) \tag{11}$$

$$G = \frac{1}{2}E_f(\varepsilon_{cr})^2\pi h_f g(\alpha,\beta,\frac{\sigma_s}{\sigma_s^y},\frac{E_s^t}{E_s}) \tag{12}$$

where $g(\alpha,\beta)$ and $g(\alpha,\beta,\frac{\sigma_s}{\sigma_s^y},\frac{E_s^t}{E_s})$ are calculated using finite element method, and α and β are Dundur's parameters. During the continuous loading process (before the nucleation of a new crack), the ERR increases. Once the ERR achieves or exceeds the fracture toughness Γ_{cr}, it is assumed the new crack will nucleate. The fracture toughness is a material constant, once obtained we can use it to predict the general fracture behavior of the material system. To the authors' knowledge, there is neither standard test procedure nor standard methodology for measurement of fracture toughness of thin films. One estimation method is using the crack onset strain to calculate the fracture toughness. For the TiO_2/PET film we are studying, the crack initiated at a very low strain level, 0.42%, where interlayer and substrate are both under elastic deformation. Eq. 11 can be used to estiamte the fracture toughness by inserting ε_{cr} = 0.42% and solving for Γ_{cr}. Table 1 lists the materal properties of the TiO_2/PET material system, with the PET parameters taken from measurements on 76.2 μm un-aged uncoated PET film. The properties of TiO_2 are obtained from the database of *AZO Materials*. The calculated fracture toughness is 20.62 J/m^2. With the value of fracture toughness, we can then further predict the crack evolution behavior.

Table 1. Material properties of the TiO_2/PET system. The subscript *s* refers to the PET substrate, subscript *i* to the interface layer and the subscript *f* to the TiO_2 film.

Properties	*Values*	*Properties*	*Values*
E_f*(GPa)	*230*	E_s (GPa)	4
v_f*	*0.25*	v_s	0.4
G_i (GPa)	1.7	E_s^t (GPa)	0.2
G_i^t (GPa)	0.085	σ_s^y (GPa)	0.095
τ_i^y(GPa)	0.0548		

* TiO_2 properties from http://www.azom.com/properties.aspx?ArticleID=1179

Cracking modeling and experimental validation. Both a linear and an elastoplastic model have been utilized to predict the crack evolution of the TiO_2/PET system under uniaxial tension test, using the parameters from Table 1. Figure 4 shows the comparison of experimental data against modeling curves for crack spacing versus substrate strain. In the experimental measurement, the crack space is taken as the

average value of distances between every two parellel neighboring cracks. The number of cracks increases with the increase of strain resulting in a varying number (~10-50) of measured spacings at different deformation stages. Both modeling curves follow the trend of the data qualitatively, with a crack spacing that decreases with the increase of substrate strain. For the initial stage, the two models match with each other very well. However, once the substrate goes into plastic deformation, the curves start showing divergence where the linear model goes to flat gradually while the elastoplastic model swiches to flat immediately. Presumably, the correlation of models can be further improved through a simultaneous communication between stress-strain model and fracture model. We note that the predictions of the model shown in Figure 4 rely on material constants either taken from the literature or directly measured by us, with no fitting parameters used. Through a detailed parameter or model correlation study, the agreement between experimental and modeling results could be further improved and we could obtain more representative material constants for this material system but this is beyond the scope of this work. We also note that the viscoelastic behavior of the polymer substrate may affect the crack evolution, which could be another explanation for the divergence between our model and the experimental data for the linear stage.

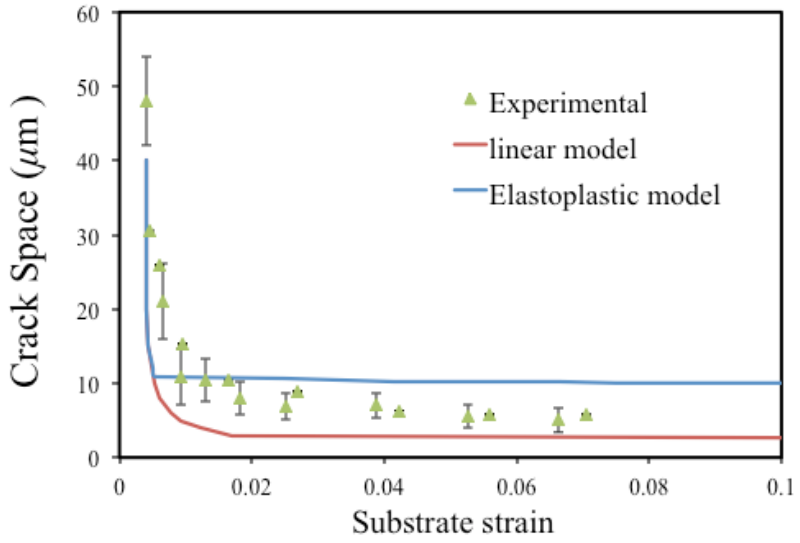

Figure 4: Comparison of crack space against substrate strain data from experimental measurement and model predictions. Representative error bars of ±1 standard deviation (~68% confidence interval) are shown for the experimental points.

EFFECT OF AGING ON THE CRACKING BEHAVIOR

Priliminary UV aging tests were conducted on the TiO_2/PET system for up to 96 hours, with the TiO_2 coating facing the light source. The coating morphology before and after aging are examined under the microcope. Figure 5(a) shows the initial coating surface morphology. A few cracks were observed which is likely due to temperature gradient induced thermal stress during the deposition process. As reported by Leterrier et al. (2003), the residual compressive strain in the coating for a

SiO_x/PET system can be 0.2~0.6%, which means the thermal stress itself can be large enough to fracture the coating.

There is not much difference observed in the surface morphology between the aged and unaged samples. However, there may be more cracks initated on the surface due to aging induced residual stresses. We note that although the aging temperature is nominally room temperature, under 10X UV exposure the temperature of the film can increase to roughly 40 °C, as detected using a thermal couple located at the substrate. It is also noticed that the UV-aged films are curved after aging. This increase of film radius indicates that UV exposure introduced additional residual stress into the film. UV aging is also found to degrade the interface strength substantially. Figure 5(b) shows the surface morphology after an adhesion test in which we bond and then peel the coating side with dry tape. On the aged sample we can see that the TiO_2 coating is peeled off from the substrate, and the resultant surface of the substrate is smooth, indicating a poor interface bonding between the TiO_2 coating and the PET substrate. A similar test repeated on the unaged sample shows that the coating layer is not removed.

Figure 5: (a) Surface morphology of unaged TiO_2/PET system, (b) Surface morphology of UV aged TiO_2/PET system after adhesion test.

Based on the experimental observations, the effect of UV aging on the cracking behavior is discussed below in terms of three aspects:

Effect of mechanical property degradation for polymer substrate. As shown in Figure 2, the UV aging converts the polymer substrate from ductile to brittle, which simplifies the fracture problem from elasto-plastic to purely elastic. Since there is negligible change of elastic properties for the polymer substrate, according to the theory equations, the crack evolution behavior of aged specimen should remain the same as that of unaged specimen until the ultimate failure strain is reached, where the aged specimen fails earlier. This indicates that the maximum crack density for an aged specimen will be much smaller and far from the saturation point. Alternatively, Eq. (10) can be utilized to convert the coating crack density data into substrate deformation. This information could be useful for inferring the mechanical loading history of a sample that was weathered under real-world conditions. Through

examining the crack distribution, we can obtain information regarding the critical environmental loading conditions (Figure 2).

Effect of interlayer properties. The effect of interlayer properties could be significant due to its impact on stress/strain profiles and fracture mechanism, as discussed by Chen et al. (2015) and illustrated in Figure 5. In case of a weak interlayer, the interface debonding initates at a relatively earlier strain level and will dominate the subsequent fracture process. In this paper, the elastoplastic model is utilized to study the deformation profiles and energy release rate of the coating layer against interface properties. As shown in Figure 6, the model (Eqs. 6-10) predicts that the normal displacement and energy release rate follow a linear relationship with the interlayer yield stress, which is consistent with the analytical solution, where parameter B has a linear relationship with τ^y. In the case of a higher yield stress, the interlayer deforms less, resulting a larger displacement variation through the thickness at the ends of the crack island and producing a larger energy release rate. This suggests that the plastic deformation of the interlayer can delay the cracking of the coating layer, or in other words, that the thin film system with a brittle interlayer may fracture more compared with that with a tough interlayer. Based on the model analysis and experimental observation in Figure 5(b), we can expect that the cracking behavior will change significantly with the increase of aging time due to changes in the interfacial bonding strength.

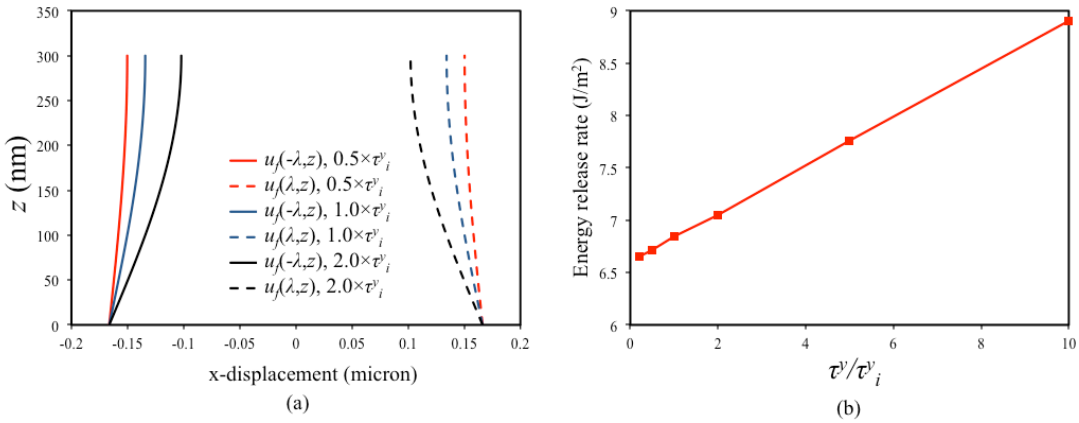

Figure 6: (a) Through-thickness displacement profile at two ends of the crack island with different interlayer yield stress values; (b) Relationship of energy release rate against interlayer yield stress (λ = 7 μm, ε =4.75%).

Effect of aging induced initial cracks. Considering the initial cracks in the form of transverse cracks aligning perpendicular to the pull direction, similar to the crack pattern shown in Figure 3, then the presence of an initial crack can be intepreted as a decrease of the initial length spanned by un-cracked coating (or crack space) of the sample. The effect of initial span on the crack onset behavior is studied using the linear elastic model combined with Eq. (10) as shown in Figure 7. As we can see, for a constant coating thickness, the crack onset strain decreases with the increase of crack space (λ), and it becomes flat when the crack space goes beyond certain critical value. For example, for h_f = 300 nm, the critical crack space is approximately 45 μm

corresponding to λ/h_f = 150. This suggests that the crack onset behavior will be affected by the aging only when the aging-induced initial crack space is lower than 45 μm. It is also noticed that the critical crack space increases with the increase of coating thickness indicating a more significant effect of aging in a thicker film.

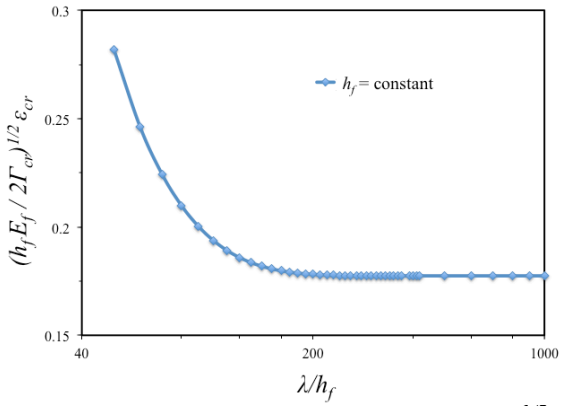

Figure 7: Normalized applied critical tensile strain $(h_f E_f/2\Gamma_{cr})^{1/2}\varepsilon_{cr}$ with respect to the crack space/coating thickness ratio.

CONCLUSION

The cracking behavior and effect of UV aging for a TiO_2 thin film bonded to a PET substrate is studied using an analytical model. The model predicts the evolution of crack space and correlates with the experimental data reasonably well. The effect of UV aging is studied in terms of three phenomena: mechanical properties degradation of polymer substrate; degradation of interlayer between substrate and oxide coating; and internal stress induced cracks on the oxide coating. The preliminary results suggest that the UV aging induced a low ultimate failure strain for the substrate and initial cracks in the coating layer but neither of these changes affects much the crack onset behavior. We find that UV aging reduces the adhesion of the TiO_2 coating to the PET substrate significantly, and the elasto-plastic model presented here predicts that the weaker adhesion has a significant effect on the cracking behavior of TiO_2 under tension.

ACKNOWLEDGMENTS

This work was supported by U.S. Department of Energy, Office of Energy Efficiency and Renewable Energy, under award number DE-FOA-0000861. We also thank Dr. Eric Benson and Dr. Suzanne Ferrere for their assistance on the fragmentation tests.

REFERENCE

Beuth, J.L. (1992) “Cracking of thin bonded films in residual tension.” *Int. J. Solids Struct.*, 29(13), 1657-1675.

Beuth, J.L. and Klingbeil, N.W. (1996) “Cracking of thin films bonded to elastic-plastic substrate.” *J. Mech. Phys. Solids*, 44(9), 1411-1428.

Chen, F.L., He, X., Prieto-Munoz, P.A. and Yin H.M. (2015) "Opening-mode fractures of a brittle coating bonded to an elasto-plastic substrate." *Int. J. Plasticity*, 67, 171-191.

DiGrazia, M.J., Jorgensen, G., Gee, R. and Bingham, C. (2012) "Service life prediction for Reflecttech® mirror film." *Proceedings of the 41st ASES National Solar Conference 2012 (Solar 2011),* Denver, CO.

Hu, M.S. and Evans, A.G. (1989) "The cracking and decohesion of thin films on ductile substrates." *Acta Metall.*, 37(3), 917-925.

Laws, N. and Dvorak, G.J. (1989) "Progressive transverse cracking in composite laminates." *J. Compos. Mater.*, 22(10), 900-916.

Letterrier, Y., Boogh, L., Andersons, J. and Manson, J.A. (1997a) "Adhesion of silicon oxide layers on poly (ethylene terephthalate). I: Effect of substrate properties on coating's fragmentation process." *J. Polym. Sci., Part B: Polym. Phys.*, 35(9), 1449-1461.

Letterrier, Y., Boogh, L., Andersons, J. and Manson, J.A. (1997b) "Adhesion of silicon oxide layers on poly (ethylene terephthalate). II: Effect of coating thickness on adhesive and cohesive strengths." *J. Polym. Sci., Part B: Polym. Phys.*, 35(9), 1463-1472.

Leterrier, Y. (2003) "Durability of nanosized oxygen-barrier coatings on polymers." *Prog. Mater. Sci.*, 48(1), 1-55.

Li, T. and Suo Z. (2006) "Deformability of thin metal films on elastomer substrates." *Int. J. Solids Struct.*, 43(7-8), 2351-2363.

Li, T. and Suo Z. (2007) "Ductility of thin metal films on polymer substrates modulated by interfacial adhesion." *Int. J. Solids Struct.*, 44(6). 1696-1705.

Oreski, G. and Wallner, G.M. (2005) "Aging mechanisms of polymeric films for PV encapsulation." *Sol. Energ.*, 79(6), 612-617.

Xia, Z. and Hutchinson, J.W. (2000) "Crack patterns in thin films." *J. Mech. Phy. Solids*, 48(6-7), 1107-1131.

Xie, C. and Tong, W. (2005) "Cracking and decohesion of a thin Al_2O_3 film on a ductile Al-5%Mg substrate." *Acta Mater.*, 53(2), 477-485.

Yanaka, M., Tsukahara, T. and Nakaso, N. (1998) "Cracking phenomena of brittle films in nanostructure composites analysed by a modified shear lag model with residual strain." *J. Mater Sci.*, 33(8), 2111-2119.

Ye, T., Suo, Z. and Evans, A.G. (1992) "Thin film cracking and the roles of substrate and interface." *Int. J. Solids Struct.*, 29(21), 2639-2648.